CrystEngComm

Accepted Manuscript

ROYAL SOCIETY OF CHEMISTRY

www.rsc.org/crystengcomm

Journal Name

RSCPublishing

Paper

Nanocrystal Formation and Polymorphism of Glycine

Cite this: DOI: 10.1039/xoxxoooooox

Xiaochuan Yang [a], Allan S. Myerson [a,*]

Received ooth January 2012,
Accepted ooth January 2012

DOI: 10.1039/xoxxoooooox

www.rsc.org/

Abstract: The surface of a crystal may play an important role in its physical and chemical properties. The percentage of molecules that are exposed on surfaces increases significantly as the crystal size decreases. However, the role of surface molecules and crystal size on the physiochemical properties of crystals is poorly understood. Here, using glycine as a model compound, nano-sized crystals were obtained by two different methods – nano spray drying and bi-functional self-assembled monolayers (SAMs). The surface structures of these nanocrystals were examined and the solubility was measured as a function of size for both the α-form and β-form. In addition, our results indicate that the solubility ratio of β-form/α-form changes as size decreases.

1. Introduction

Research on crystal surfaces at the nano and molecular scale is of great interest.[1-6] From a molecular perspective, molecules on the surface are unique. The same crystal may have different facets and molecules on the non-symmetric facets are arranged in different ways.[7] Previous work on nanocrystals has been focused on bulk properties, such as solubility and melting point, and tends to ignore crystal surface or consider molecules on the surface the same as molecules in the bulk.[8-13] This is generally correct for most cases where surface molecules contribute little. However, surface molecules play a vital role in some cases. One example is crystal growth mechanism. The way that molecules arrange themselves and grow on surfaces is poorly understood.[14] Recently, Ward and his co-workers utilized a real-time in situ atomic force microscope (AFM) and found that L-cystine dimethylester and L-cystine methylester inhibits the growth of the six symmetry-equivalent {100} steps due to specific bindings at the crystal surface.[15] Zhao et al. showed that graphene primarily grows on copper single crystal facets (100) and (111) using atomic-resolution scanning tunnelling microscopy (STM).[16] Another good example is nanocrystals. As particle size decreases, the fraction of surface molecules in a crystal increases significantly. Compared to bulk molecules, molecules on surfaces possess fewer interactions in the structure and tend to leave the surface. In order to consider the importance of surface molecules in such circumstances, the Ostwald-Freundlich equation and the Gibbs–Thomson equation were derived and can be used to roughly describe some physiochemical properties' change as particle size is reduced.[17]

Organic molecular crystals normally exhibit more crystal defects than inorganic crystals.[18] Most organic molecules form molecular crystal structures by intermolecular and intramolecular forces. Compared to ionic and covalent bonds, the intermolecular forces in molecular crystals are generally weak, including electrostatic interaction between dipoles, dispersion forces and hydrogen bonds.[13] In addition, compared to atoms or ions in many often-discussed metallic or ionic crystals, most organic molecules are non-simply shaped and exhibit low degree symmetry. Therefore, organic solids show more complex structures and are generally harder to crystallize. Crystal defects are easily incorporated into the structure, especially near the surface.[13, 18]

The role of surface molecules and crystal size on the physiochemical properties of organic molecular nanocrystals is poorly understood. In this work, we selected glycine as the model compound. Glycine is one of the simplest organic molecules, and exhibits six different polymorphs.[19] Three of them can be obtained at room temperature and pressure (α, β and γ). The other three were obtained under high pressure.[20, 21] Their stability order is $\gamma > \alpha > \beta$. For crystals above 1 micron, were surface molecules do not have a significant influence on bulk properties, the ratio of the solubility of polymorphs is a constant for any solvent at a given temperature.[22] It is the goal of this work to determine if this is also the case for crystals below one micron, where surface molecules have an increasing importance on properties such as solubility.

2. Experimental Section

Materials: Glycine (ReagentPlus®, ⩾ 99%) and water (CHROMASOLV® Plus) were obtained from Sigma Aldrich and 200 proof ethanol was obtained from VWR.

Experimental Setup (Figure 1): Patterned gold substrates with island size 1 μm were prepared in MIT microsystems technology laboratories. The experimental setup can be generalized into three steps. First silicon substrate was patterned by photolithography, then coated with 5 nm titanium layer and 50 nm gold layer. The rest of the photoresist were stripped off by immersing the substrates in acetone for 2 hours. After being cleaned and dried with a nitrogen gun, the substrates with gold islands were ready to prepare bi-functional self-assembled monolayers (SAMs).

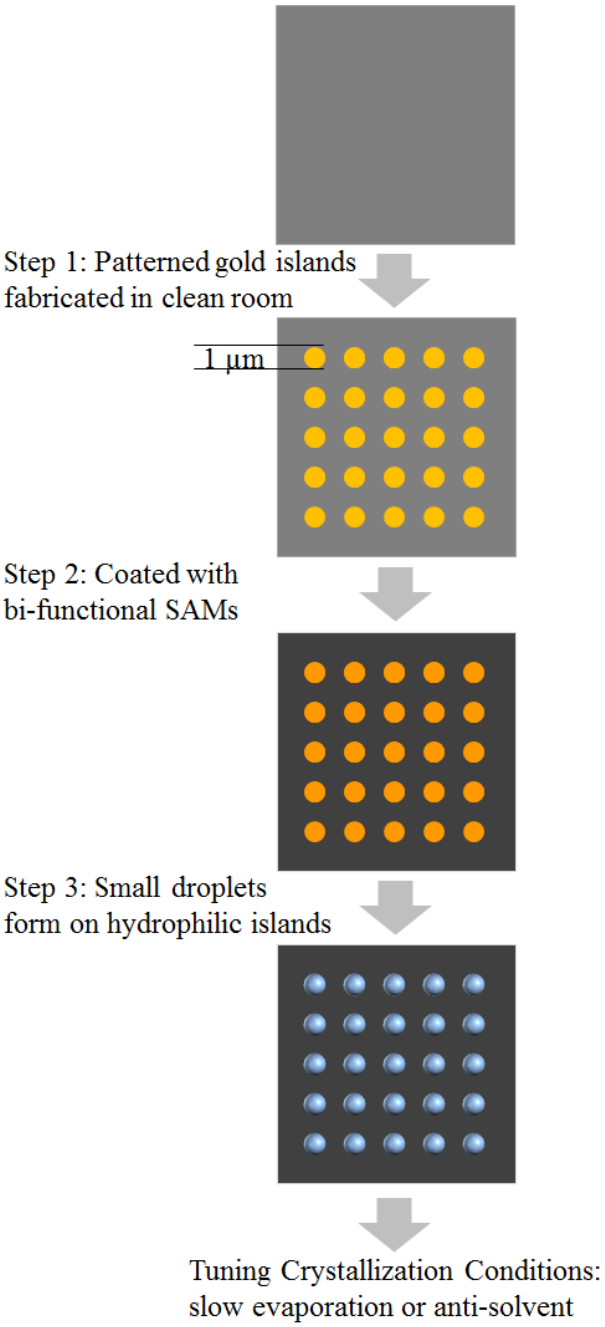

Figure 1 Illustration of steps to achieve droplet crystallization on bi-functional SAMs substrates. More details can be found in supporting information.

Fabricated substrates with patterned gold islands as mentioned above were cleaned with piranha solution (A typical mixture of 3:1 concentrated sulfuric acid to 30% hydrogen peroxide solution) for 20 minutes for the cleaning of all organic impurities from the surface. Substrates were then washed with copious amount of pure water and isopropanol then dried with a nitrogen gun. Cleaned patterned substrates were slowly put into a 10 mM thiol/ethanol (3-mercaptopropionic acid, 3MPA) solution in pure nitrogen atmosphere for 18 hours for the formation of hydrophilic SAMs on gold islands, i.e. –COOH group of 3MPA exposing outwards. Substrates were rinsed three times with pure ethanol and dried with nitrogen gas and immersed into a 2 mM OTS (n-Octadecyltrichlorosilane)/toluene solution for 40 minutes for the formation of hydrophobic SAMs on the remaining silicon surface. After being rinsed 3 times with pure toluene and dried with nitrogen gas, the bi-functional SAMs substrates were ready with hydrophilic thiol on gold islands and hydrophobic OTS on the remaining silicon area for the crystallization of glycine. Surfaces were scanned under Atomic Force Microscope (AFM). The roughness of these gold island surfaces were at most ±2 nm. These bi-functional SAMs substrates were then used under different slow evaporation and anti-solvent crystallization conditions to obtain the desired polymorphic outcome. More details can be found in supporting information and the experimental section of our previous work.[6]

Raman analysis: We used Horiba Jobin-Yvon Labram HR800 spectrometer equipped with a 514 nm line using 1800 grooves/mm and a 100x microscope objective. One benefit of gold islands is that the Raman signal is enhanced due to the surface-enhanced effect by gold. The characteristic peaks 2972/3008 cm^{-1} for α-form, 2953/3010 cm^{-1} for β-form and 2964/3000 cm^{-1} for γ-form were used for polymorph characterization.

X-Ray Powder Diffraction (XRPD) analysis: The instrument (X'Pert PRO, PANalytical Inc.) is equipped with a PW3050/60 standard resolution goniometer and a PW3373/10 Cu LFF DK241245 X-ray tube. The high tension generator high voltage and anode current were set as 45 kv and 40 mA when using. A spinner sample stage PW3064 (Reflection mode) was used for all the samples. Settings on incident beam path include: soller slit 0.04 rad., mask fixed 10 mm, programmable divergence slit and fixed 1° anti-scatter slit. Settings on diffracted beam path include: soller slit 0.04 rad. and programmable anti-scatter slit. The scan was programmed as a continuous scan: 2θ angle 2-40°, step size 0.0083556°, time per step 19.685 s; three repeated scans were collected to average. The XRPD patterns obtained for each sample can be used to calculate the relative amounts of polymorphs in the sample. The mass ratio of different polymorphs is proportional to the ratio of the corresponding characteristic crystalline peak areas.[23, 24]

Solubility measurement: Glycine/ethanol solutions of different supersaturated concentrations were carefully prepared just before we tested the solubility of nanocrystals. Glycine was recrystallized to eliminate possible impurities in commercial bottles. Ethanol and the solutions were filtered with 0.2 μm Whatman® Anotop syringe filters before use. The solubility of bulk glycine crystals in ethanol at 25 °C was measured using gravimetric methods to be 0.263 ± 0.015 mg glycine/g solution for α-form and 0.309 ± 0.008 mg glycine/g solution for β-form. To prepare a solution of supersaturation S = 1.1, for example, we put 0.34 g glycine into 1000 g ethanol and stirred the slurry on a hot plate. We gradually increased the temperature until crystals were fully dissolved. Then we raised the temperature by another 5 °C and held it for another 30 minutes.. The supersaturated solutions normally remained clear for at least 2 hours. Solubility was tested by putting a sample in a supersaturated solution of a given concentration and determining if the crystals dissolved. The same crystal (Its polymorph was already confirmed by the Raman analysis) was checked under the Atomic Force Microscope before and after the test. If it does not dissolve, the same sample was added to a supersaturated solution of a lower concentration. This was continued until the sample dissolved. The averaged concentration of the last two solution used was considered as the solubility for that size.

3. Results and discussion

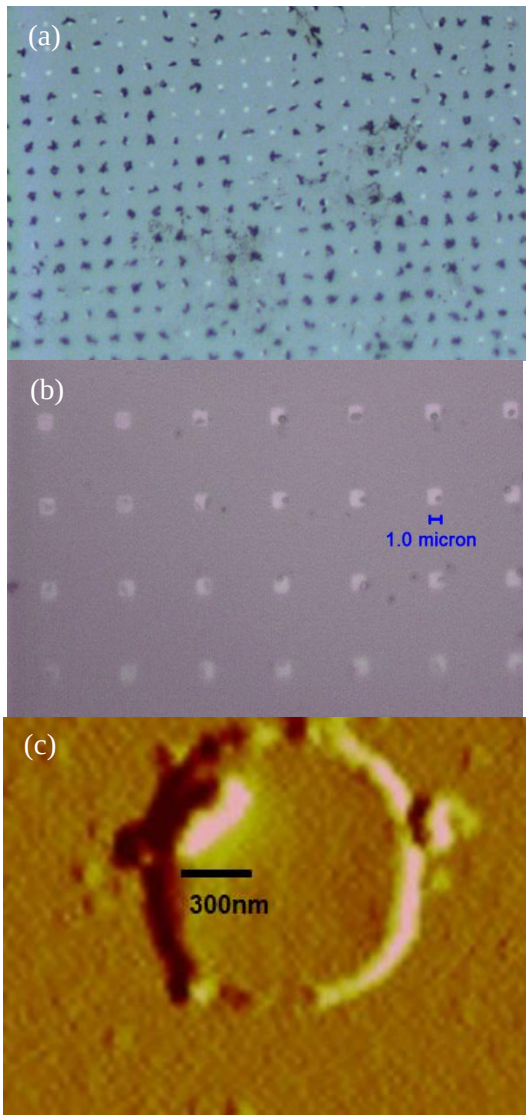

Figure 2 Images of nanocrystals formed on bi-functional SAMs substrates. (a) Nanocrystals from a glycine/water solution of 0.207 g glycine/g solution. Black dirt was photoresist residue left. (b) Nanocrystals from a glycine/water solution of 0.011 g glycine/g solution. (c) One of the nanocrystals in (b) under AFM.

Previously we have shown the use of substrates of 1μm gold islands coated with bi-functional Self-Assembled Monolayers (SAMs) for the production of nano-sized mefenamic acid crystals with controlled polymorphs as small as ~ 300 nm.[6] Here we utilized the same technique to produce nanocrystals of different glycine polymorphs. Instead of varying surface chemistry, we controlled polymorphic outcome by changing solution pH and crystallization conditions (slow diffusion of anti-solvent or slow evaporation[6]). Figure 2a shows glycine nanocrystals on 1 μm gold islands from a glycine/water solution of 0.207 g glycine/g solution. The largest dimension of these nanocrystals is from 683 nm to 1.19 μm. Unlike nanocrystals formed using nano spray drying, most of the nanocrystals here clearly showed needle-like shapes as shown in Figure 2a. Figure 2b shows glycine nanocrystals on 1 μm gold islands from a glycine/water solution of 0.011 g glycine/g solution. Due to the limit of focus depth of optical microscope, the left region of the image is blurry but one dot per island is clear. The crystal size is already under wavelength of visible light, and is probably almost the same as resolution limit of that objective lens in the microscope. . Figure 2c shows an AFM resolution image of one of the nanocrystals, and a crystal-like shape rather than a sphere can be easily distinguished. These results suggest that the nano-crystallization process under these experimental conditions is slow and the actual crystal structure of the individual nanocrystals is much better organized than that of individual nanocrystals formed by spray drying (See below). It is inferred that more distortions and defects existing in the spray dried nanocrystals, and the existence and extent of these distortions and defects may be substantially affected by the crystallization techniques. There is a possibility that distortions also exist inside the crystals, but we did not have proper tools to confirm this. Formation of a defect free crystal is quite challenging and may not be possible particularly for crystals below 1 micron. The largest dimension of these nanocrystals is from 210 nm to 418 nm.

Previous work in our laboratory obtained mostly β-glycine nanocrystals.[25, 26] Here, we successfully obtained mostly α-glycine when we waited for a longer time (more than a month), and varied the surface chemistry (hydrophilic SAMs with -COOH) and island sizes. Solubility vs size curves of both polymorphs were measured with results shown in Figure 3. Compared to the bulk solubility, 286 ± 25 nm α-glycine nanocrystals showed 19.8% increase and 229 ± 32 nm β-glycine nanocrystals exhibited 16.4% enhancement in solubility. Using the Ostwald-Freundlich equation surface tensions for α-glycine and β-glycine were calculated to be 2729 and 1826 erg/cm^2 (2.729 and 1.826 N/m), respectively. However, we are not certain that these values can represent nanocrystals with 100% well-ordered structures. Those two fitted curves will cross at r = 97 nm, indicating that β-glycine is more stable than α-glycine due to the effect of surface molecules when the crystal size is under 97 nm. Similar results on the same order of magnitude of size-dependent stability of polymorphs were reported on organic molecular crystals such as anthranilic acid.[27, 28] The metastable form II persisted in 7.5 nm pores and was believed to possess a smaller cluster size.

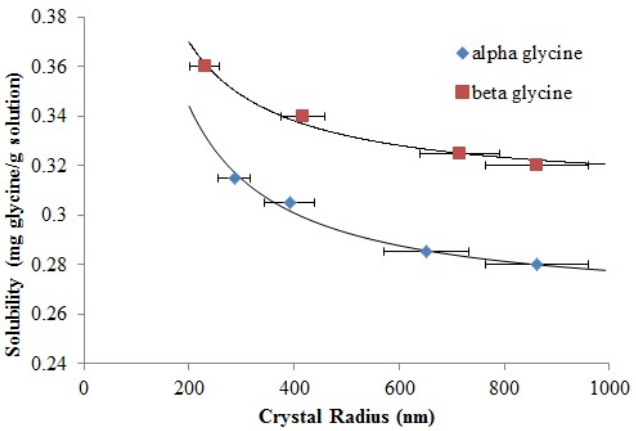

Figure 3 Solubility curve of different polymorphs of glycine. Two black lines are fitted curves using the Ostwald-Freundlich equation (R^2 = 0.981 for α-glycine and 0.983 for β-glycine).

We also used Buchi nano spray dryer (model B-90) to obtain glycine nanocrystals. The smallest spray mesh (hole diameter is 4.0 μm) was used in all experiments. A glycine/water solution was sprayed from a spraying head through the mesh, and solvent evaporates for crystallization during falling of droplets. The role of experimental conditions, such as solution concentration, pH and temperature, on the size and polymorphic outcome were explored as shown in Table 1. In many cases, we see concomitant nucleation of

at least two polymorphs. This is consistent with literature.[25, 29, 30] As temperature decreases and pH changes to acidic/basic, more stable forms (α and γ) start to show. As solution concentration decreases, size reduction of product particles was not obvious. It can be explained by the relationship between a particle's diameter (d) and its volume (V): d is proportional to $V^{1/3}$ ($d \sim V^{1/3}$). However, the particle's volume (V) is proportional to the solution concentration (C) ($V \sim C$), assuming the volume of one droplet coming from the mesh is the same for each spraying. Therefore, the relationship is $d \sim C^{1/3}$. Even when the solution concentration decreased to 1/5 of its original value, the particle size only reduces to 58% of its original value.

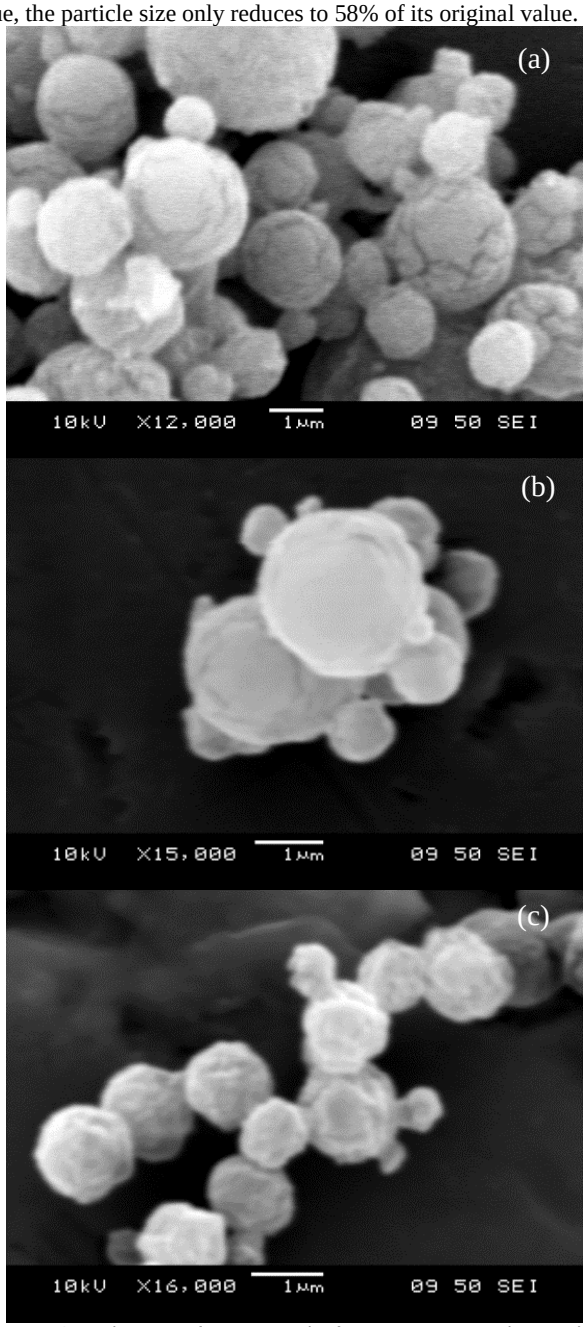

Figure 4 SEM images of nanocrystals from nano spray dryer using a glycine/water solution (0.021 g/g solution) at 95 °C. A 20-nm gold layer was coated. (a) and (b) were images taken immediately after the spraying. (c) was taken 2 hours after the spraying.

Figure 4 shows the result of spraying a glycine/water solution (0.021 g/g solution) at 95 °C. The size of particles exhibits a wide distribution from ~ 200 nm to ~ 3 μm, indicating that droplets coming from the mesh are quite different in size. The shapes of these particles are spherical without any obvious crystal facets. The particles are possibly not single crystals but many crystalline domains. As one droplet falls, free fall movement takes 0.45 seconds to pass a distance of 1 meter. When solvent evaporates in such a short time, it is possible that multiple nucleation events occur, or many defects are generated during crystal growth even when there is only one nucleus. Interestingly, we did not observe any amorphous solid in the XRPD analysis which was conducted immediately after spraying. Figure 4c is the image of the same sample which was taken 2 hours after the other two images. One noticeable change is that these crystals start to form connections with adjacent crystals. The sample was stored under ambient conditions which were tested to be 23°C and 35%RH. From the molecular perspective, glycine molecules, especially those on the surface of particles, showed very high mobility. It is strongly related to the poorly ordered crystal structure at the surface. This "crystal-bridging" phenomenon indicates that these nanocrystals formed using nano spray dryer are not stable when they are piled together and possess a high tendency to form bigger crystals through the "crystal-bridging". These nanocrystals, nonetheless, cannot be tested for solubility vs size. Although number based percentage of crystals of size < 1 μm are more than half, volume based percentage of those are at most 20%. When we put the sample into a solution of a given concentration, it is hard to visually distinguish whether the crystals dissolve or not.

Table 1 Polymorphic outcome of glycine nanocrystals formed using spraying analyzed by XRPD.

Glycine/water solution (0.106 g glycine/g solution)			
	pH = 2	pH = 6	pH = 10
T = 75 °C	18% α, 82% β	13% α, 87% β	α, β, γ (18:47:35)
T = 95 °C	100% β	100% β	α, β, γ (7:82:11)
Glycine/water solution (0.021 g glycine/g solution)			
	pH = 2	pH = 6	pH = 10
T = 75 °C	α, β, γ (13:68:19)	21% α, 79% β	α, β, γ (10:52:38)
T = 95 °C	12% α, 88% β	15% α, 85% β	α, β, γ (14:80:6)

4. Conclusion

Crystal surfaces are a vital part of organic molecular nanocrystals. Through nano spray drying, we obtained spherical nanocrystals with disordered surface structures. These defects on crystal surfaces may significantly enhance mobility of molecules and therefore larger crystals form by "crystal-bridging". In addition, by using bi-functional SAMs substrates, we obtained glycine nanocrystals with narrow size distributions and controlled polymorph. We found that the solubility ratio of β-glycine/α-glycine changes as crystal size decreases. Recent work reported by other investigators demonstrated melting point depression of nanocrystals and size-dependent stability of polymorphs under confinement.[27, 28, 31-34] To the best of our knowledge, no one has reported similar findings for organic molecular nanocrystals which are unconfined. Our results help further understand the importance of surface molecules in organic molecule crystals nanocrystals.

Notes and references

[a] Department of Chemical Engineering, Massachusetts Institute of Technology, 77 Massachusetts Avenue, Cambridge, MA 02139, USA

Electronic Supplementary Information (ESI) available: details of experimental set-up and calculated XRPD patterns of glycine. See DOI: 10.1039/c000000x/

1. I. Halasz and H. Vančik, *CrystEngComm*, 2011, **13**, 4307.
2. Y. Diao, A. S. Myerson, T. A. Hatton and B. L. Trout, *Langmuir : the ACS journal of surfaces and colloids*, 2011, **27**, 5324-5334.
3. Y. Diao, T. Harada, A. S. Myerson, T. A. Hatton and B. L. Trout, *Nat Mater*, 2011, **10**, 867-871.
4. A. D. Daigle and J. J. BelBruno, *Surface Science*, 2011, **605**, 1313-1319.
5. K. Chadwick, J. Chen, A. S. Myerson and B. L. Trout, *Crystal Growth & Design*, 2012, **12**, 1159-1166.
6. X. Yang, B. Sarma and A. S. Myerson, *Crystal Growth & Design*, 2012, **12**, 5521-5528.
7. C. P. Price, A. L. Grzesiak and A. J. Matzger, *Journal of the American Chemical Society*, 2005, **127**, 5512-5517.
8. X. Yang, T.-C. Ong, V. K. Michaelis, S. Heng, J. Huang, R. G. Griffin and A. S. Myerson, *CrystEngComm*, 2014.
9. Q. Jiang and M. D. Ward, *Chemical Society reviews*, 2014, **43**, 2066-2079.
10. M. Wang, G. C. Rutledge, A. S. Myerson and B. L. Trout, *Journal of pharmaceutical sciences*, 2012, **101**, 1178-1188.
11. A. Safaei, *The Journal of Physical Chemistry C*, 2010, **114**, 13482-13496.
12. J. Ba, J. Polleux, M. Antonietti and M. Niederberger, *Advanced Materials*, 2005, **17**, 2509-2512.
13. A. S. Myerson, *Handbook of Industrial Crystallization*, Butterworth-Heinemann, 2002.
14. R. Mohan and A. S. Myerson, *Chem Eng Sci*, 2002, **57**, 4277-4285.
15. J. D. Rimer, Z. An, Z. Zhu, M. H. Lee, D. S. Goldfarb, J. A. Wesson and M. D. Ward, *Science*, 2010, **330**, 337-341.
16. L. Zhao, K. T. Rim, H. Zhou, R. He, T. F. Heinz, A. Pinczuk, G. W. Flynn and A. N. Pasupathy, *Solid State Communications*, 2011, **151**, 509-513.
17. W. Wu and G. H. Nancollas, *Journal of solution chemistry*, 1998, **27**, 521-531.
18. D. S. Chemla, *Nonlinear optical properties of organic molecules and crystals*, Elsevier, 2012.
19. S. V. Goryainov, E. V. Boldyreva and E. N. Kolesnik, *Chemical Physics Letters*, 2006, **419**, 496-500.
20. E. Boldyreva, S. Ivashevskaya, H. Sowa, H. Ahsbahs and H.-P. Weber, Doklady Physical Chemistry, 2004.
21. A. Dawson, D. R. Allan, S. A. Belmonte, S. J. Clark, W. I. David, P. A. McGregor, S. Parsons, C. R. Pulham and L. Sawyer, *Crystal Growth & Design*, 2005, **5**, 1415-1427.
22. T. L. Threlfall, *Analyst*, 1995, **120**, 2435-2460.
23. S. N. Campbell Roberts, A. C. Williams, I. M. Grimsey and S. W. Booth, *Journal of Pharmaceutical and Biomedical Analysis*, 2002, **28**, 1149-1159.
24. Y. Diao, K. E. Whaley, M. E. Helgeson, M. A. Woldeyes, P. S. Doyle, A. S. Myerson, T. A. Hatton and B. L. Trout, *Journal of the American Chemical Society*, 2011, **134**, 673-684.
25. K. Kim, A. Centrone, T. A. Hatton and A. S. Myerson, *Crystengcomm*, 2011, **13**, 1127-1131.
26. K. Kim, I. S. Lee, A. Centrone, T. A. Hatton and A. S. Myerson, *Journal of the American Chemical Society*, 2009, **131**, 18212-+.
27. J. M. Ha, J. H. Wolf, M. A. Hillmyer and M. D. Ward, *J. Am. Chem. Soc.*, 2004, **126**, 3382.
28. J. M. Ha, B. D. Hamilton, M. A. Hillmyer and M. D. Ward, *Crystal Growth & Design*, 2009, **9**, 4766-4777.
29. A. Singh, I. S. Lee and A. S. Myerson, *Crystal Growth & Design*, 2009, **9**, 1182-1185.
30. I. S. Lee, A. Y. Lee and A. S. Myerson, *Pharmaceutical research*, 2008, **25**, 960-968.
31. Q. Jiang, C. Hu and M. D. Ward, *Journal of the American Chemical Society*, 2013, **135**, 2144-2147.
32. B. D. Hamilton, M. A. Hillmyer and M. D. Ward, *Crystal Growth & Design*, 2008, **8**, 3368-3375.
33. J. M. Ha, M. A. Hillmyer and M. D. Ward, *The Journal of Physical Chemistry B*, 2005, **109**, 1392-1399.
34. D. Knezic, J. Zaccaro and A. S. Myerson, *Crystal Growth & Design*, 2004, **4**, 199-208.

Table of Contents:

We obtained α-/β-glycine nanocrystals, examined their surface structures and found the solubility ratio of β-form/α-form changes as size decreases.